GLIA 45:17–27 (2004)

Characterization of Lysophosphatidic Acid and Sphingosine-1-Phosphate-Mediated Signal Transduction in Rat Cortical Oligodendrocytes

NAICHEN YU,* KAREN D. LARIOSA-WILLINGHAM, FEN-FEN LIN, MICHAEL WEBB, AND TADIMETI S. RAO

Molecular Neuroscience, Merck Research Laboratories, San Diego, California

KEY WORDS lysophospholipid receptors; lysophosphatidic acid; sphingosine-1-phosphate; oligodendrocytes; receptors; G-protein; MAP kinase; protein kinase C; phospholipase C; calcium

ABSTRACT Lysophosphatidic acid (LPA) and sphingosine-1-phosphate (S1P) have been proposed to play a key role in oligodendrocyte maturation and myelinogenesis. In this study, we examined lysophospholipid receptor gene expression in differentiated rat oligodendrocyte cultures and signaling downstream of lysophospholipid receptor activation by LPA and S1P. Differentiated oligodendrocytes express mRNAs encoding lysophospholipid receptors with the relative abundance of *lpa1* > *s1p5* > *s1p1* = *s1p2* = *lpa3* > *s1p3*. LPA and S1P transiently increased phosphorylation of extracellular signal-regulated kinase (ERK) with EC_{50} values of 956 and 168 nM, respectively. LPA- and S1P-induced ERK phosphorylation was dependent on the activation of mitogen-activated protein kinase (MAPK), phospholipase C (PLC), and protein kinase C (PKC), but was insensitive to pertussis toxin (PTX). LPA increased intracellular calcium levels in oligodendrocytes and these increases were partially blocked by a PLC inhibitor but not by PTX. In contrast, S1P was not found to induce measurable changes of intracellular calcium. These results taken together suggest that lysophospholipid receptor activation involves receptor coupling to heterotrimeric G_q subunits with consequent activation of PLC, PKC, and MAPK pathways leading to ERK phosphorylation.

INTRODUCTION

Lysophosphatidic acid (LPA) and sphingosine-1-phosphate (S1P) are endogenous bioactive phospholipid agonists of a family of G-protein-coupled lysophospholipid receptors (lpR), previously described as endothelial differentiation gene (Edg) receptors. So far, eight members of the family have been discovered in mammalian cells: *lpa1*, *lpa2*, and *lpa3* receptors for LPA (formerly known as Edg-2, Edg-4, and Edg-7, respectively), and *s1p1*, *s1p2*, *s1p3*, *s1p4*, and *s1p5* receptors for S1P [formerly known as Edg-1, Edg-5, Edg-3, Edg-6, and Edg-8, respectively; for reviews of nomenclature, see Chun et al. (2002)].

LPA induces a variety of biological actions, including proliferation, differentiation, survival, and chemotaxis (Moolenaar, 1995; Tokumura, 1995). LPA receptors couple to three out of four primary classes of heteromeric G-proteins, $G_{i/o}$, G_q, and $G_{12/13}$, but not to G_s. Activation of LPA receptors results in wide spectrum of intracellular events, such as increases in inositol phosphates and intracellular calcium (An et al., 1998), inhibition of adenylyl cyclase (Hecht et al., 1996; Tigyi et al., 1996; Arimura et al., 1998), activation of kinases such as protein kinase C (PKC) (Seewald et al., 1999; Kim et al., 2000; Paolucci et al., 2000; Rui et al., 2000),

*Correspondence to: Dr. Naichen Yu, Merck Research Laboratories, 3535 General Atomics Court, Building 1, San Diego, CA 92121.
E-mail: naichen_yu@merck.com

Received 16 January 2003; Accepted 28 May 2003

DOI 10.1002/glia.10297

mitogen-activated protein kinase (MAPK) (Hordijk et al., 1994; Takeda et al., 1998, 1999), and Rho kinase (Buhl et al., 1995; Ramakers and Moolenaar, 1998). Ample biological evidence shows involvement of distinct G-protein coupling mechanisms in specific signal transduction pathway(s). For example, the mitogenic action of LPA is almost completely inhibited by pertussis toxin (PTX), implicating the critical involvement of $G_{i/o}$ (Grey et al., 2001), whereas the LPA-induced stress-fiber formation and cell rounding responses through Rho activation appear to involve $G_{12/13}$ (Buhl et al., 1995).

Mechanistic studies of S1P receptor signal transduction are facilitated by the availability of transfected cell lines expressing single subtypes of S1P receptors. *S1p1* couples to $G_{i/o}$ and its activation stimulates MAPK (Zondag et al., 1998; Gonda et al., 1999; Lee et al., 1999), inhibits adenylyl cyclase (Lee et al., 1998; Okamoto et al., 1998; Zondag et al., 1998), and activates phospholipase C (PLC), leading to calcium mobilization (Okamoto et al., 1998). *S1p2* couples to $G_{q/11}$ (Kon et al., 1999; Windh et al., 1999) and receptor activation leads to PLC activation with resulting increases in inositol phosphates and intracellular calcium (Gonda et al., 1999). S1P-induced cell proliferation, survival, and related signaling events are mediated by *s1p3* and *s1p2* (An et al., 2000), whereas S1P inhibits proliferation and extracellular signal-regulated kinase (ERK) 1/2 activities in Chinese hamster ovary cells expressing *s1p5* (Malek et al., 2001).

Lpa1 is the first G-protein-coupled receptor (GPCR) found to be selectively expressed in myelin-forming cells in the nervous system and its temporal expression pattern is consistent with its role in neurogenesis during embryonic development and in myelination during postnatal life (Allard et al., 1998). In situ hybridization studies have shown that *lpa1* is concentrated in and around developing white matter tracts of postnatal mouse brain and is coexpressed with proteolipid protein (PLP), a marker for mature oligodendrocytes (Weiner et al., 1998). Immunohistochemical studies also show that *lpa1* proteins are prominently expressed in the white matter track region of adult rat brain (Cervera et al., 2002) and cultured oligodendrocytes (Handford et al., 2001) and is colocalized with myelin basic protein (MBP) (Cervera et al., 2002). Interestingly, mRNA for *s1p5* is also found predominantly in white matter tracts of rat brain such as corpus callosum, optic nerve, and olfactory tract and the white matter of cerebellum (Im et al., 2000). These unique distribution patterns of *lpa1* and *s1p5* suggest that lpRs might play an important role in fundamental functions of oligodendrocytes, such as myelination, and that modulation of the receptors could be a therapeutic strategy for demyelinating diseases such as multiple sclerosis (MS).

Although there is a wealth of literature on receptor distribution and mechanistic studies of signal transduction of LPA and S1P receptors in non-CNS tissues, our knowledge about the effects of these bioactive lysophospholipids on myelinating cells in the brain or in the periphery is still limited. LPA has been shown to be a potent survival factor for cultured Schwann cells (Weiner and Chun, 1999) and modulator of calcium signals (Möller et al., 1999) and ERK1/ERK2 activation (Stankoff et al., 2002) in cultured oligodendrocytes. S1P also induces ERK2 activation in rat oligodendrocytes (Hida et al., 1999). However, there are few comparative studies of the signal transduction pathways of LPA and S1P in oligodendrocytes. Therefore, we investigated the comparative mRNA distribution of LPA and S1P receptors and signaling events downstream of receptor activation, such as increases in intracellular calcium and in phosphorylated ERK (pERK), as well as on excitatory amino acid-evoked cell injury in well-characterized cultures of rat oligodendrocytes.

MATERIALS AND METHODS

Cell Culture

All the culture and assay reagents were purchased from Sigma (St. Louis, MO) unless stated otherwise. Primary mixed glial cultures were prepared from Sprague-Dawley rats (0–2 days old) and grown in Dulbecco's modified Eagle medium (DMEM; Life Technologies, Rockville, MD) supplemented with 25 mM glucose, 2 mM L-glutamine, and 10% heat-inactivated fetal bovine serum (FCS; Omega Scientific, Tarzana, CA) at 37°C in incubator with 5% CO_2 for 10–14 days. After initiation, the culture media were changed 6 days later and twice a week thereafter. The oligodendrocyte/type-2 astrocyte (O-2A) progenitors and microglia were separated from type 1 astrocytes by shaking the cultures at 350 rpm at 37°C overnight (15–17 h) as originally described (McCarthy and Vellis, 1980). The purification, proliferation, and differentiation of oligodendrocytes were performed by published methods (Bögler et al., 1990; Canoll et al., 1996) with minor modifications. Briefly, the detached O-2A progenitors and microglia were replated onto nontissue culture-treated flasks and allowed to adhere in the incubator for 2–3 h. During this process, microglia attach firmly to the surface while the O-2A progenitors attach loosely and were detached by gentle flushing and replating onto poly-L-lysine-coated 6-well or 48-well tissue culture plates. The isolated cells were incubated for 2–3 h and media were replaced by DM^+ (DMEM supplemented with 40 ng/ml selenium, 0.3 μg/ml tri-iodothyronine, 5 μg/ml bovine insulin, 100 μg/ml human transferrin, 60 ng/ml progesterone, 16 μg/ml putrescine, 0.4 μg/ml thyroxine, 2 mM glutamine, and 0.5% heat-inactivated FCS) freshly supplemented with 10 ng/ml platelet-derived growth factor (PDGF; Roche Diagnostics, Indianapolis, IN) and 10 ng/ml basic fibroblast growth factor (bFGF; Roche Diagnostics). The cultures were grown at 37°C in 8% CO_2 for 7–10 days. The culture media were replaced by fresh DM^+ for 2 days and then DMEM for 1 day to allow differentiation before the cells were used for assays.

TABLE 1. Sequences of Primers and Probes and Constructs of Minigenes

Gene	Accession #	Forward primer (F)/TaqMan probe (TM)/reverse primer (R)	Minigenes
lpa1	AF090347	F: 5′-GACACCATGATGAGCCTTCTGA TM: 5′-AAAGGCACCCAGCACAATGACCACA R: 5′-CCCGGAGTCCAGCAGACA	pCR-Blunt II-rLPA1
lpa3	AF097733	F: 5′-CACACGAGTGGCTCCATCAG TM: 5′-CTCCTAAGACAGTCATCACCGTCTTCATTAGCTTC R: 5′-GGTCCAGCACACCACGAA	pCRII-TOPO-rLPA3
slp1	U10303	F: 5′-CTGACCTTCCGCAAGAACATCT TM: 5′-CAAGGCCAGCCGCAGTTCCG R: 5′-CTTCAGCAAGGCCAGAGACTTC	pCR2.1-TOPO-rLPB1
slp2	AF022138	F: 5′-GCCTTGTACGTCCGAATCTACTTC TM: 5′-TAGTCCGCTCAAGCCATGCGGAC R: 5′-AGCGTCTGAGGACCAGCAA	pCR2.1-TOPO-rLPB2
slp3	AF184914	F: 5′-ACGCGCGCATCTACTTCCT TM: 5′-CCACCCTGCGGCTGCTGGACT R: 5′-TGGATCTCTCGGAGTTGTGGTT	pCR-Blunt II-rLPB3
slp5	AF233649	F: 5′-CTCTAGAGCGCCACCTTACCAT TM: 5′-CAGGCGGCCACCGCCATC R: 5′-CCCAGCAGCAGCGACAA	pCRII-TOPO-rLPB4
β-actin	V01217	F: 5′-ATGCCCCGAGGCTCTCTT TM: 5′-CCTTCCTTCCTGGGTATGGAATCCTGTG R: 5′-CTTCATGATGGAATTGAATGTAGTTTC	
β-actin	V01217	F: 5′-GCTATGAGCTGCCTGACGGT R: 5′-GTACTTGCGCTCAGGAGGAG	pCR-Blunt II-rβ-actin

Immunostaining and Cell Counting

Purity of oligodendrocyte cultures was established by immunofluorescence analysis by using antibody against galactocerebroside (GalC), a marker for mature oligodendrocytes. Cells were briefly washed with phosphate-buffered saline (PBS) before fixation in 4% paraformaldehyde for 20 min at room temperature. Fixed cells were blocked by 10% FCS in PBS. Primary anti-GalC antibody of rabbit serum was used at 1:50 and goat-antirabbit antibody conjugated with Alexa 488 (Molecular Probes, Eugene, OR) was used at a dilution of 1:50. To determine the percentage of GalC-positive cells, immunostained oligodendrocytes were counterstained by 4′,6-diamidino-2-phenylindole, dihydrochloride (DAPI; Molecular Probes) at a concentration of 5 μg/ml. The cells were viewed with an Olympus BX60 epifluorescence microscope and the images were collected by a digital camera.

RNA Analysis

Isolation of total RNA and reverse transcription

Total RNA from adult rat whole brain was isolated using a ToTally RNA kit (Ambion, Austin, TX). For further removal of genomic DNA contamination, total RNA was treated with RNase-free DNase I on RNeasy midi columns and purified using an RNeasy Protect Midi kit (Qiagen, Valencia, CA). Total RNA from differentiated oligodendrocytes was isolated using an RNeasy Protect Midi kit. One μg of total RNA was reverse-transcribed using RETROscript kit (Ambion). In each reverse transcription reaction, a reaction of omitting reverse transcriptase was included for the assessment of genomic DNA contamination.

Cloning, construction, and DNA sequencing of minigenes for lpRs and β-actin

The cDNAs encoding *lpa1*, *lpa3*, *s1p1*, *s1p2*, *s1p3*, *s1p5*, and β-actin were amplified from rat brain with polymerase chain reaction (PCR) techniques. Primers used for these genes were designed from sequences in the Genebank database (Table 1). For cloning of *lp*R minigenes, cDNA (2 μl) was amplified using 10 pmol of each primer and TaqMan Universal PCR Master Mix (25 μl) in a total volume of 50 μl. PCR was performed using a GeneAmp 9700 thermocycler (ABI, Foster City, CA) with incubation at 50°C for 2 min, 95°C for 10 min, followed by 40 cycles of 15 s at 95°C and 1 min at 60°C. β-actin minigene was amplified with 2.5 U of PfuTurbo DNA polymerase (Stratagene, La Jolla, CA), 200 nM dNTP, and 10 pmol of each primer, in a total volume of 50 μl for 30 cycles in GeneAmp 9700 thermocycler (ABI). Each cycle consisted of 30 s at 95°C, 30 s at 55°C, and 45 s at 75°C. The PCR-amplified fragments were subcloned into PCR cloning vectors, pCR-Blunt II-TOPO or pCR II-TOPO (Invitrogen, Carlsbad, CA) using PCR Cloning Kit (Invitrogen; Table 1). The integrity of these genes was confirmed by sequencing using an ABI 3100 automated fluorescence sequencer (ABI). The sequence was analyzed using software Sequencer.

TaqMan PCR

TaqMan PCR was carried out using an ABI Prism 7900 sequence detector on 1 μl of cDNA samples using 900 nM of each primer, 250 nM TaqMan probe, and 25 μl of TaqMan Universal PCR Master Mix, in a total volume of 50 μl. PCR was executed with incubation at 50°C for 2 min, 95°C for 10 min, followed by 40 cycles at 95°C for 15 s and at 60°C for 1 min. Additional reac-

tions were performed in 96-well plate using known dilutions of DNA from minigenes as PCR template for constructing a standard curve relating threshold cycle to cDNA concentration. Data were analyzed using software SDS2.0. All measured PCR products were corrected based on the amount of β-actin cDNA, and all data were normalized to β-actin and expressed as % β-actin.

Western Blotting Analysis

After the removal of the medium, cells were washed in warm DMEM and exposed to pharmacological treatments in warm (37°C) DMEM containing 1% fatty acid-free BSA for preselected time points. At the end of the exposure, media were aspirated and the cultures were rinsed once with 4 ml Earle's Balanced Salt Solution (EBSS). Cells were lysed in 300 μl NP-40 lysis buffer containing protease inhibitor cocktail containing 10 mM NaF, 1 mM Na_3VO_4, and 1 mM PMSF. Cell lysates with 5 μg protein were separated on a 4–20% Tris HCl Criterion Precast Gel (Bio-Rad, Hercules, CA) and transferred onto Hybond ECL nitrocellulose membrane (Amersham Pharmacia Biotech, Piscataway, NJ). After transfer, membranes were blocked with PBS with 0.1% Tween-20 and 5% (W/V) milk powder overnight at 4°C, incubated with the primary antibodies (p44/42 MAP kinase or phospho-p44/42 MAP kinase, 1:1,000; Cell Signaling, Beverly, MA) overnight at 4°C, followed by an incubation with HRP-conjugated secondary antibody (1:10,000; Amersham Pharmacia Biotech) for 2 h at room temperature. Bands were visualized by treatment with SuperSignal West Femto Maximum Sensitivity Substrate (Pierce, Rockford, IL) followed by exposure to Kodak BIOMAX ML film (Eastman Kodak, Rochester, NY)

Measurement of $[Ca^{2+}]_i$ by Fluo-4AM Using Fluorescence Plate Reader

Intracellular calcium measurements by Fluo-4AM (Molecular Probes) were performed as previously described (Manning and Sontheimer, 1999) with minor modifications. Oligodendrocytes grown in 96-well plates were washed with assay buffer (EBSS supplemented with 20 mM HEPES, 10 μM glycine, and 40 μM probenecid) and incubated with Fluo-4-AM (10 μM in assay buffer; 100 μl/well) at 32°C for 2 h. After the dye was removed, cells were washed gently with 200 μl of assay buffer to remove any dye nonspecifically associated with the cell surface and incubated with 100 μl of assay buffer containing 0.1% fatty acid-free BSA in the FLUOstar Galaxy (BMG LabTechnologies, Durham, NC) plate carrier at room temperature for 15 min to allow deesterification of the intracellular AM ester. Test reagents (100 μl, 2× concentration) were delivered to oligodendrocytes in assay buffer containing 0.1% fatty acid-free BSA and fluorescence intensities were measured for 40 s, after which F_{max} and F_{min} calibrations for quantitative Ca^{2+} measurements were performed. Data were expressed as peak/basal ratio by plotting changes in Ca^{2+} (peak) as a function of time calibrated relative to the basal Ca^{2+} levels.

Toxicity Assay

Oligodendrocytes were exposed to insult [α-amino-3-hydroxy-5-methy-4-isoxazolepropionic acid (AMPA) and cyclothiazide (CTZ)] or in conjunction with LPA for 2 h in EBSS at 37°C. At the end of the insult, supernatants were collected and the cells were lysed by EBSS containing 0.1% Triton X-100. Aliquots of supernatants and lysates (25 μl) were used to measure lactate dehydrogenase (LDH) by Cytotoxicity Detection Kit (Boehringer Mannheim, Indianapolis, IN). The results were expressed as percentage of LDH efflux.

Data Analysis

All values are expressed as mean ± standard error of mean (SEM). For statistical evaluation, analysis was done with analysis of variance (ANOVA) followed by Neuman-Keuls test as a posthoc test using software GraphPad Prism 3.0 (San Diego, CA) to compare possible difference among various treatment groups.

RESULTS

Establishment of Cultures of Differentiated Oligodendrocytes

As a prerequisite to investigate the effects of LPA and S1P on oligodendrocytes, we first established and characterized differentiated oligodendrocyte cultures as described previously (Bögler et al., 1990; Canoll et al., 1996). Progenitor cells expanding in DM^+ supplemented with PDFG and bFGF initially have a bipolar morphology (not shown) and become multipolar after withdrawal of PDGF and bFGF. Differentiated oligodendrocytes were characterized by an increased number of highly ramifying processes (Fig. 1A), accompanied by the expression of GalC, a marker for mature oligodendrocytes. The GalC immunoreactivity was concentrated in the cell bodies and to a lesser extent in the processes (Fig. 1B). Microscopic analysis of nearly 600 cells in seven random fields from two independent experiments indicated that 97.5% (580 out of 595) of DAPI-labeled cells were GalC-positive (Fig. 1C).

Expression of *Lpa* and *S1p* Receptors in Differentiated Oligodendrocytes

We have employed a highly sensitive and quantitative TaqMan PCR method to examine the distribution of mRNA. We exploited the six existing rat sequences

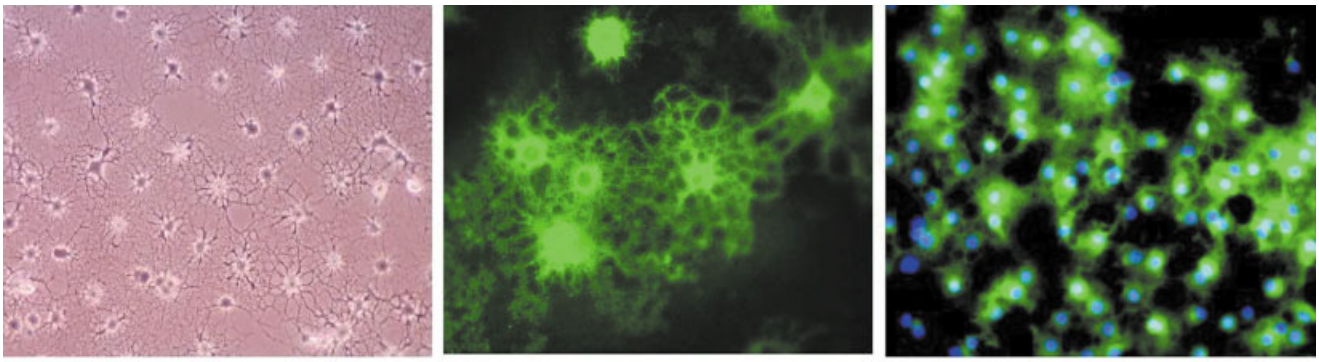

Fig. 1. Characterization of mature rat cortical oligodendrocytes. Phase contrast micrograph (**A**) and immunofluorescence staining of GalC (**B**) and immunofluorescence staining of GalC counterstained with DAPI (**C**) are shown. Cells were cultured in DM^+ supplemented with PDGF and bFGF for 7 days and changed to DM^+ for 2 days before phase contrast microscopy (magnification in A, 100×). Cells were processed for immunofluorescence staining with primary anti-GalC antibody and secondary antibody conjugated with Alexa 488. All the cells in the field were GalC-positive (magnification in B, 200×); 97.5% of; DAPI-labeled cells (595) are GalC-positive cells (580). Data from seven random fields (magnification in C, 100×) of two independent cultures.

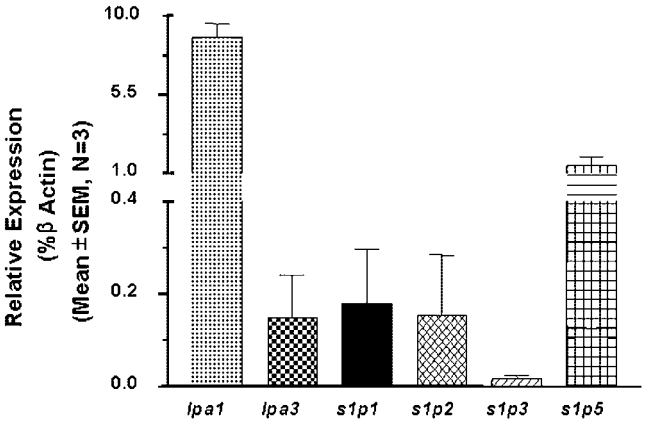

Fig. 2. LpR mRNA expression profile in differentiated rat cortical oligodendrocytes. Data represent expression of individual lpR mRNA relative to β-actin whose expression was normalized to 100. The rank order of the expression was *lpa1* > *s1p5* > *s1p1* = *s1p2* = *lpa3* > *s1p3*. *Lpa1* level was respectively 6-, 49-, 57-, and 58-fold higher than *s1p5*, *s1p1*, *s1p2*, and *lpa3* mRNA expression, while *s1p3* mRNA was expressed at a very low level. Among four *s1ps* tested, *s1p5* has the highest level of expression while *lpa2* and *s1p4* were not investigated since the rat sequences were not currently available.

for lpRs to quantify the levels of expression of those receptors in cultured oligodendrocytes with β-actin as the reference gene for normalization purposes. As shown in Figure 2, in three independent oligodendrocyte preparations, six lpRs were found with the following rank order of gene expression: *lpa1* > *s1p5* > *s1p1* = *s1p2* = *lpa3* > *s1p3*. The mRNA for *lpa1* was the most abundant and was 6-, 49-, 57-, and 58-fold higher than those of *s1p5*, *s1p1*, *s1p2*, and *lpa3*, respectively. The mRNA for *s1p3* was the least abundant of all. Among four *s1ps* tested, *s1p5* showed the highest level of expression. The expression profiles of *lpa1* and *s1p5* in mature oligodendrocyte cultures were complemented by in situ hybridization analysis, which showed that *lpa1* (Weiner et al., 1998) and *s1p5* (Im et al., 2000) were expressed in postnatal murine and rat brain white matter, respectively.

Transient and Concentration-Dependent Activation of pERK by LPA and S1P

LPA has been shown to phosphorylate pERK1/pERK2 in a murine hepatocyte cell line AML12 (Sautin et al., 2001) and in rat oligodendrocytes (Stankoff et al., 2002). To test the abilities of LPA and S1P to activate MAPK pathways, we used antibodies, which selectively recognize nonphosphorylated or phosphorylated forms of ERK to differentiate between inactive and activated ERK. A fixed concentration of LPA or S1P (2 μM) was applied to differentiated oligodendrocytes for various lengths of time (1–60 min). Both LPA and S1P increased ERK phosphorylation with detectable changes seen as early as 1 min, peaking at 10 min, which gradually decreased to near basal levels by 60 min (Fig. 3). LPA, at the tested concentration (2 μM), resulted in greater ERK phosphorylation than S1P (40–50% of maximal effects by LPA). The pharmacology of LPA- and S1P-induced ERK phosphorylation was examined with a 10-min agonist treatment. LPA and S1P produced concentration-dependent increases in pERK with EC_{50} values of 956 and 168 nM, respectively. LPA was consistently more efficacious than S1P in this response (Fig. 4).

LPA- and S1P-Mediated pERK Activation Is Not PTX-Sensitive

In order to clarify which G-proteins are involved in LPA- or S1P-induced pERK activation, oligodendrocytes were treated with PTX (200 ng/ml, 18–24 h) before application of LPA or S1P. As shown in Figure 5, PTX treatment did not significantly change the basal levels of

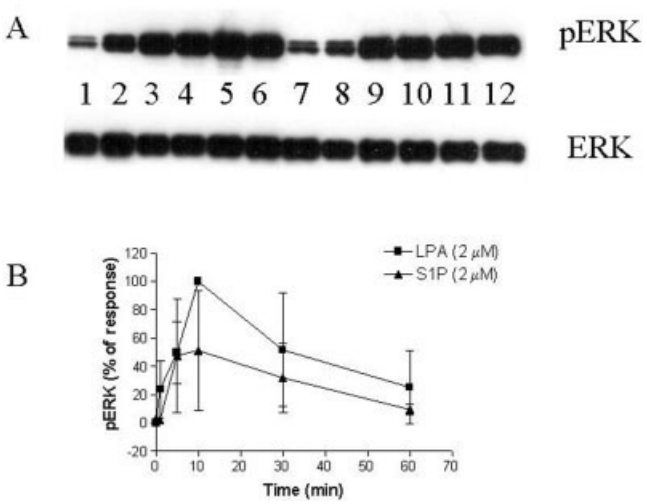

Fig. 3. Time course of LPA or S1P on activation of pERK. After the application of agonists for various periods of time, cells were lysed and both ERK and pERK were measured by Western blotting. Representative Western blots of ERK and pERK are shown in lower and upper panels in **A**, respectively. Lane 1, CTR; lane 2, LPA 1 min; lane 3, LPA 5 min; lane 4, LPA 10 min; lane 5, LPA 30 min; lane 6, LPA 60 min; lane 7, CTR; lane 8, S1P 1 min; lane 9, S1P 5 min; lane 10, S1P 10 min; lane 11, S1P 30 min; lane 12, S1P 60 min. **B:** Intensities of individual bands were determined by densitometric scanning (Personal Densitometer SI, Molecular Dynamics) and analyzed by ImageQuant software (Molecular Dynamics). Ratios of digitized pERK and ERK signals were calculated and used to normalize pERK activities. The response value of LPA at 10 min was used as 100%. Values represent mean ± SEM from three independent experiments.

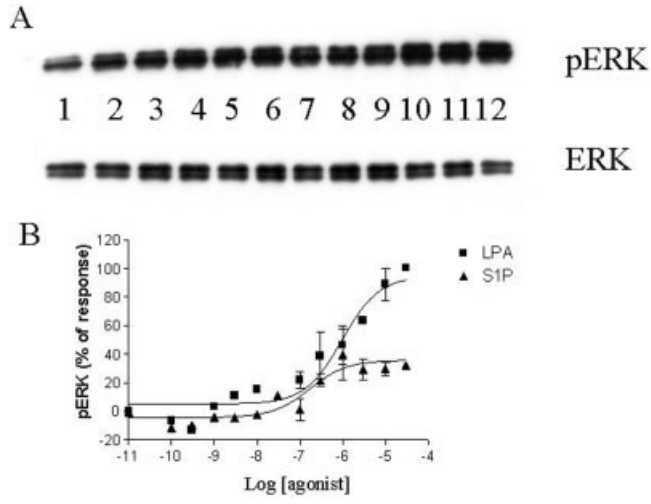

Fig. 4. Concentration response curves of LPA or S1P on pERK activation. After application of agonists at various concentrations for 10 min, cells were lysed and both ERK and pERK were measured by Western blotting. Representative Western blots of ERK and pERK are shown in lower and upper panels in **A**, respectively. Lane 1, CTR; lane 2, S1P 0.3 μM; lane 3, S1P 1 μM; lane 4, S1P 3 μM; lane 5, S1P 10 μM; lane 6, S1P 30 μM; lane 7, LPA 0.1 μM; lane 8, LPA 0.3 μM; lane 9, LPA 1 μM; lane 10, LPA 3 μM; lane 11, LPA 10 μM; lane 12, LPA 30 μM. **B:** Intensities of individual bands were determined by scanning densitometry (Personal Densitometer SI, Molecular Dynamics) and analyzed by ImageQuant software (Molecular Dynamics). Ratios of digitized pERK and ERK signals were calculated and used to normalize pERK activities. Response values of LPA at 30 μM were used as 100%. Values represent mean ± SEM from five independent experiments. EC_{50s} were 956 and 168 nM for LPA and S1P, respectively.

pERK, nor did it modify the responses to LPA or S1P. The magnitude of the LPA response by PTX-pretreated oligodendrocytes was very similar to that observed in cells without PTX pretreatment. Although the magnitude of S1P responses in PTX-pretreated oligodendrocytes appeared to be slightly higher than those without PTX, these differences did not reach statistical significance.

LPA- and S1P-Mediated ERK Phosphorylation Is Completely Abolished by PLC, PKC, or MAPK Inhibitors

We investigated the roles of PLC and MAPK in lysophospholipid-induced pERK activation. Most widely used PLC inhibitor (U73122, 30 μM) and MAPK inhibitor (PD98059, 10 μM) were added to oligodendrocytes 10 min prior to LPA or S1P application. Both inhibitors significantly reduced pERK basal levels (Fig. 6). More importantly, both U73122 and PD98059 completely blocked LPA- or S1P-induced pERK activation while ERK levels were not affected (Fig. 6). Similarly, chelerythrine chloride (10 μM), an inhibitor of the substrate binding to the catalytic domain of PKC, completely abolished LPA- or S1P-induced pERK activation, suggesting that activation of PKC is upstream of the ERK phosphorylation pathway (Fig. 7). Chelerythrine chloride also significantly reduced pERK basal levels but not ERK levels (Fig. 7).

Sensitivity of LPA-Induced $[Ca^{2+}]_i$ Responses to PLC Inhibitor

To investigate the involvement of PLC in lysophospholipid signaling in oligodendrocytes, we utilized a Fluo-4-based assay to measure intracellular calcium. LPA (1 μM) increased $[Ca^{2+}]_i$ up to 20% over basal levels, which reached maximal levels over a period of 40 s. In contrast, we were unable to see consistent and measurable increases in intracellular calcium following the application of 1 μM S1P (not shown). With a view to understanding the pharmacology of LPA-induced increases in intracellular calcium, we examined its sensitivity to PTX and U73122. PTX pretreatment (200 ng/ml, 18–24 h) did not attenuate LPA-induced $[Ca^{2+}]_i$ elevation (Fig. 8), suggesting a lack of involvement of $G_{i/o}$-coupled mechanisms in this response. However, U73122 (10 μM) attenuated LPA-induced $[Ca^{2+}]_i$ by ~ 50% (Fig. 8), implicating activation of the PLC pathway by LPA, which in turn causes internal calcium release.

Lack of Effects of LPA on AMPA/CTZ-Induced Excitotoxicity

As oligodendrocytes have been shown to be vulnerable to AMPA/kainate receptor-mediated excitotoxicity in vivo (McDonald et al., 1998) and in vitro (Mat-

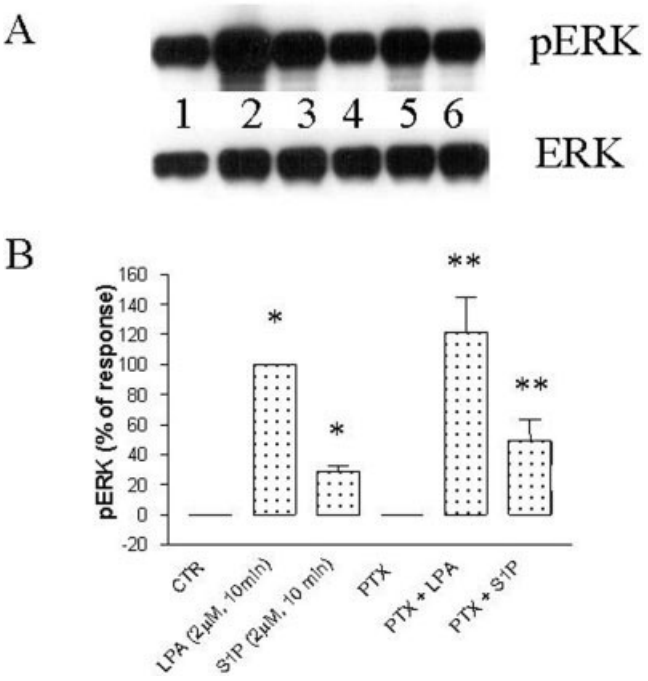

Fig. 5. LPA- and S1P-induced pERK activation is PTX-insensitive. Oligodendrocytes were subjected to PTX treatment (200 ng/ml, 18–24 h) before agonists were applied (2 μM, 10 min). The cells were lysed and both ERK and pERK were measured by Western blotting. Representative Western blots of ERK and pERK are shown in lower and upper panels in **A**, respectively. Lane 1, CTR; lane 2, LPA 2 μM; lane 3, S1P 2 μM; lane 4, PTX; lane 5, PTX + LPA; lane 6, PTX + S1P. **B:** Intensities of individual bands were determined by scanning densitometry (Personal Densitometer SI, Molecular Dynamics) and analyzed by ImageQuant software (Molecular Dynamics). Ratios of digitized pERK and ERK signals were calculated and used to normalize pERK activities. Response value of LPA at 2 μM was used as 100%. Values represent mean ± SEM from five independent experiments. Asterisk, $P < 0.001$ compared to CTR; double asterisk, $P > 0.05$ compared to LPA or S1P, respectively, by ANOVA followed by Neuman-Keuls test.

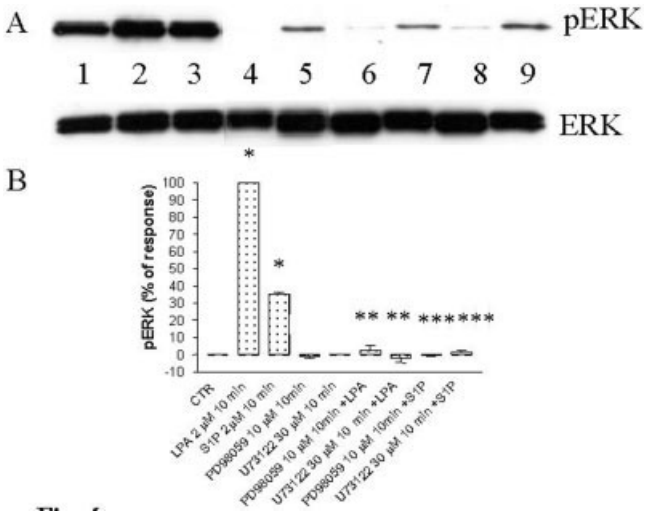

Fig. 6. MAPK and PLC are involved in LPA- and S1P-induced pERK activation. Inhibitors were added to oligodendrocytes 10 min before agonists were applied (2 μM, 10 min). The cells were lysed and both ERK and pERK were measured by Western blotting. Representative Western blots of ERK and pERK are shown in lower and upper panels in **A**, respectively. Lane 1, CTR; lane 2, LPA 2 μM; lane 3, S1P 2 μM; lane 4, PD98059 10 μM; lane 5, U73122 30 μM; lane 6, PD98059 + LPA; lane 7, U73122 + LPA; lane 8, PD98059 + S1P; lane 9, U73122 + S1P. **B:** Intensities of individual bands were determined by scanning densitometry (Personal Densitometer SI, Molecular Dynamics) and analyzed by ImageQuant software (Molecular Dynamics). Ratios of digitized pERK and ERK signals were calculated and used to normalize pERK activities. Response values of LPA at 2 μM were used as 100%. Values represent mean ± SEM from three independent experiments. Asterisk, $P < 0.001$ compared to CTR; double asterisk, $P < 0.001$ compared to LPA; triple asterisk, $P < 0.001$ compared to S1P, respectively, by ANOVA followed by Neuman-Keuls test.

ute et al., 1997) and LPA has been shown to promote Schwann cell survival (Weiner and Chun, 1999), we tested if LPA protected oligodendrocytes against AMPA/CTZ-induced excitotoxicity. First, we tested various concentrations of AMPA in conjunction with a fixed concentration of CTZ (100 μM) and found that 25 μM AMPA produced submaximal excitotoxicity (data not shown). We chose 25 μM AMPA with 100 μM CTZ as an insult paradigm to test the efficacy of LPA. As shown in Figure 9, coapplication LPA, ranging from 10 nM to 10 μM, did not prevent AMPA/CTZ-evoked excitotoxicity reflected by LDH efflux.

DISCUSSION

The expression patterns of lpR family members in differentiated oligodendrocytes were investigated by a sensitive TaqMan PCR technique. We were particularly interested in *lpa1*, since the expression of this receptor has been reported to be high in oligodendrocytes. Our results indeed confirm that differentiated oligodendrocytes express high levels of *lpa1* mRNA. Immunohistochemical studies (Handford et al., 2001; Cervera et al., 2002) demonstrated the presence of *lpa1* protein in oligodendrocytes and the present findings complement this result at the mRNA levels. Furthermore, we believe that this is the first report to detect transcripts of *lpa3* in differentiated oligodendrocytes. *S1p5* mRNA, although expressed sixfold lower than that of *lpa1*, was the most abundant species of the *s1p* family in oligodendrocytes. Our results confirm other studies in which *s1p5* mRNA is found prominently in white matter tracts of rat brain such as corpus callosum, optic nerve, olfactory tract, and white matter of cerebellum (Im et al., 2000), regions where oligodendrocytes are abundant. The relative abundance of mRNA of *lpa1* and *s1p5* in cultured oligodendrocytes is in agreement with their distribution described in the literature from in *vivo* studies. Transcripts for *s1p1* and *s1p2* were expressed at relatively lower levels while *s1p3* was just above the detection limits. This pattern of distribution of transcripts of *lpa* and *s1p* receptors in oligodendrocytes contrasts with that seen in astrocytes (Rao et al., 2003), where the rank order of abundance of mRNA was $s1p3 > s1p \geq lpa1 > s1p2 = lpa3$ with essentially undetectable levels for *s1p5*. These differences may provide in some degree the mo-

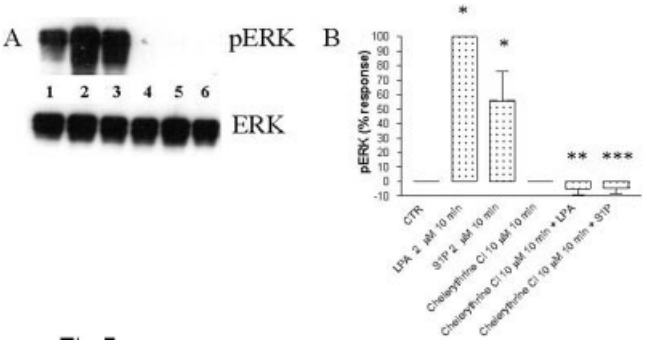

Fig. 7. PKC is involved in LPA- and S1P-induced pERK activation. Chelerythrine Cl (10 μM) was added to oligodendrocytes 10 min before agonists were applied (2 μM, 10 min). The cells were lysed and both ERK and pERK were measured by Western blotting. Representative Western blots of ERK and pERK are shown in lower and upper panels in **A**, respectively. Lane 1, CTR; lane 2, LPA; lane 3, S1P; lane 4, Chelerythrine Cl; lane 5, Chelerythrine Cl + LPA; lane 6, Chelerythrine Cl + S1P. **B:** Intensities of individual bands were determined by scanning densitometry (Personal Densitometer SI, Molecular Dynamics) and analyzed by ImageQuant software (Molecular Dynamics). Ratios of digitized pERK and ERK signals were calculated and used to normalize pERK activities. Response value of LPA at 2 μM was used as 100%. Values represent mean ± SEM from three independent experiments. Asterisk, $P < 0.001$ compared to CTR; double asterisk, $P < 0.001$ compared to LPA; triple asterisk, $P < 0.001$ compared to S1P, respectively, by ANOVA followed by Neuman-Keuls test.

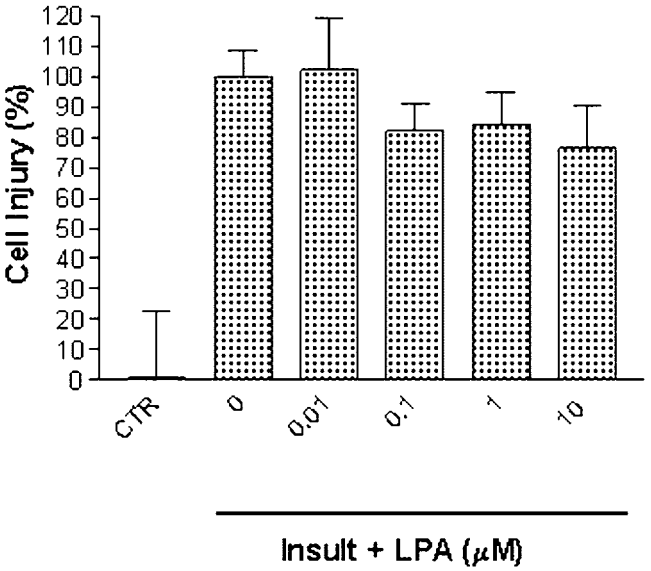

Fig. 9. Lack of oligodendrocyte protection by LPA in AMPA-mediated injury. Various concentrations of LPA were added in conjunction with the insult (25 μM AMPA and 100 μM CTZ). After 2 h of incubation, LDH was measured as described in text. Cell injury defined by LDH efflux caused by insult was expressed as 100%. Values represent mean ± SD from two independent experiments.

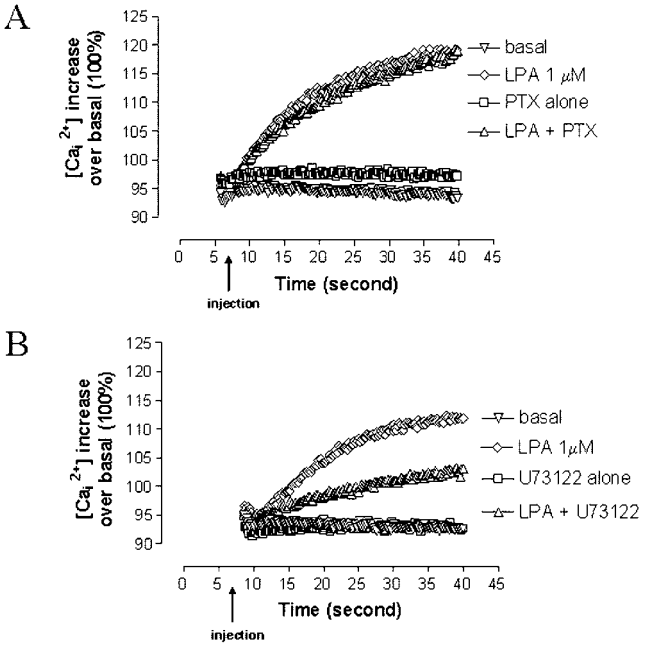

Fig. 8. Differential responses and pharmacology of LPA on intracellular calcium in oligodendrocytes. **A:** LPA induced elevation of $[Ca^{2+}]_i$. Pretreatment of oligodendrocytes with pertussis toxin (PTX 200 ng/ml, 18–24 h) did not significantly change LPA-evoked influx of calcium. Values represent mean of three independent experiments. **B:** Pretreatment of oligodendrocytes with U73122 (10 μM, 10 min prior to LPA application) partially blocked LPA-evoked calcium influx. Values represent mean of three independent experiments.

lecular basis for the differential responses by LPA and S1P between oligodendrocytes and astrocytes (Rao et al., 2003) at receptor level.

Although most cells contain small amounts of LPA associated with the membrane biosynthesis, significant amounts of extracellular LPA are derived from activated platelets, which account for the LPA in serum. LPA concentrations in brain are normally low but could potentially become higher when the blood-brain barrier is compromised in diseases such as MS. TNFα, a proinflammatory cytokine believed to play an important role in MS, has been shown to increase S1P as a result of activation of phospholipase A_2 and consequent activation of sphingomyelinase (Kim et al., 1991; Jayadev et al., 1994).

In a number of cellular systems, LPA increases ERK phosphorylation. For example, LPA phosphorylates p90RSK at Ser381, a phosphorylation site for ERK1/2 in AML12 hepatocytes with maximal effects at 5 min, declining after 45 min (Sautin et al., 2001). In this study, we demonstrated that exogenous application of LPA and S1P increased pERK activation in oligodendrocytes in a time- and concentration-dependent manner (Fig. 4). It is apparent that LPA is more efficacious than S1P. The maximal efficacy of S1P was 28% of the maximal response to LPA (Fig. 4). However, S1P is more potent than LPA, with EC_{50} values of 168 and 956 nM, respectively. The EC_{50} value for the LPA-induced ERK phosphorylation in oligodendrocytes was close to the range of EC_{50} values of 378, 998, and 214 nM reported for LPA in calcium assays in cell lines expressing *lpa1*, *-2*, and *-3*, respectively (Fischer et al., 2001). Based on the fact that *lpa1* expression levels are six times higher than those of *s1p5* (Fig. 3), it is plausible to speculate that these expression differences underlie the efficacy differences.

The lpRs couple to distinct GPCR subunits in a cell type-specific manner. The coupling of GPCRs to $G_{i/o}$ subunits is largely inferred from the sensitivity of ligand-induced signaling events to PTX. For example, LPA-induced pERK1/2 activation in mouse striatal astrocytes (Pébay et al., 1999), activation of $P21^{ras}$ in Rat-1 cells (van Corven et al., 1993), ras-dependent activation of MAP kinase pathway (Crespo et al., 1994), and S1P-induced activation of pERK in human aortic endothelial cells (Kimura et al., 2000) striatal astrocytes (Pébay et al., 2001) are all sensitive to PTX and therefore considered to be mediated through $G_{i/o}$ subunits. On the other hand, S1P-induced activation of c-Jun N-terminal kinase or p38 is totally insensitive to PTX (Gonda et al., 1999) and this is interpreted to reflect coupling to non-$G_{i/o}$ subunits. LPA- and S1P-induced ERK phosphorylation in oligodendrocytes was largely PTX-insensitive. Our results therefore favor the possibility that G-proteins other than $G_{i/o}$, such as G_q, may play a major role in pERK activation. The lack of effect of PTX sensitivity of LPA- and S1P-induced pERK activation in oligodendrocytes contrasts with the PTX sensitivity in astrocytes (Rao et al., 2003) and further underscores cell type-specific lpR coupling to G-protein subunits. GPCRs can activate MAP kinase signaling cascades by a wide variety of mechanisms such as activation of classical second messengers, coupling of G-protein subunits to novel effectors, and direct receptor coupling to effectors independent of G-proteins. GPCRs through transactivation of receptor kinases can also influence the MAP kinase pathway. Despite considerable diversity of signaling events leading up to MAP kinase activation culminating in ERK phosphorylation, activation of mitogenic pathways appears to be a common downstream event leading to cell proliferation and differentiation. Activation of the MAPK pathway by lpRs suggests that these receptors may regulate oligodendrocyte proliferation and differentiation.

It is generally agreed that G_q-dependent activation of ERKs is most commonly mediated by PLC and/or PKC. G_q directly activates PLCβ, which cleaves phosphatidyl inositol 4,5-bisphosphate (PIP2), to produce diacylglycerol (DAG) and inositol triphosphate (IP3). DAG and intracellular calcium released as a result of IP3 production activate PKCs. The role of PKC in oligodendrocyte proliferation, differentiation, and process extension was largely inferred through the use of PKC activators such as phorbol esters or PKC inhibitors such as H7, BIM, and CPG 41251 or downregulation by long-term treatment with phorbol ester or its analogue such as phorbol dibutyrate. Such studies implicate a complex role of PKC on oligodendrocyte proliferation and differentiation (Stariha and Kim, 2001). Our own results indicate that differentiated oligodendrocytes possess a basal level of PKC and PLC activities. Pharmacological inhibition of these pathways appears to affect basal ERK phosphorylation (Figs. 6 and 7). These findings are supported by the results from a previous study (Khorchid et al., 1999) that U73122 (30-min treatment) or phorbol 12-myristate 13-acetate (PMA; overnight treatment) significantly reduced the basal levels of $p42^{mapk}$ in oligodendrocyte progenitors.

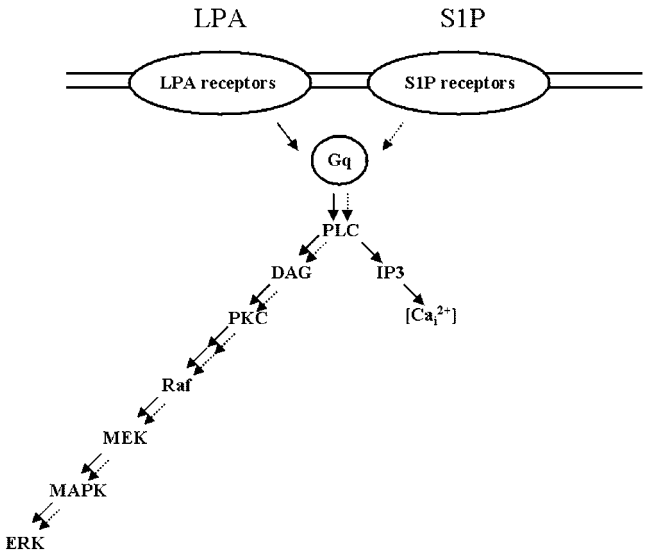

Fig. 10. Schematic diagram of possible signaling pathways involved in LPA receptor (predominantly LP_{A1}) and S1P receptor (predominantly $S1P_5$) activation by their respective ligands in rat oligodendrocytes. Straight line, pathways by LPA; dashed line, pathways by S1P.

Activation of PLC and PKC pathways by LPA or S1P has been consistently demonstrated in many other cell types. LPA-mediated PKC activation has been shown in vascular smooth muscle cells (Seewald et al., 1999) and osteoblast-like cells (Caverzasio et al., 2000) and LPA-mediated PLC activation has been shown in cultured lens epithelial cells (Ohata et al., 1997). S1P has been shown to activate PKC in rat-2 cells (Kim et al., 2000) and PLC in rat hepatocytes (Im et al., 1997). To our knowledge, this is the first report to demonstrate that LPA- and S1P-evoked ERK activation in rat cortical oligodendrocytes involves PLC as well as PKC pathways. Blocking either of the two pathways is sufficient to abolish LPA- and S1P-induced pERK activation. Our results therefore support the following signaling events in oligodendrocytes: lpR activation → G_q → PLC → DAG → PKC → → Raf → MEK → MAPK → ERK (Fig. 10).

Studies in which LPA receptor subtypes were overexpressed in host cell lines, such as *lpa1*-null neuroblastoma B103, or hepatoma RH777 revealed the existence of significant redundancy in signal transduction (Contos et al., 2000). LPA caused adenylyl cyclase inhibition in *lpa1* cell line (Hecht et al., 1996), *lpa2* cell line (An et al., 1998), and *lpa3* cell line (Ishii et al., 2000). Similarly, activation of *lpa1*, *lpa2* (An et al., 1998), and *lpa3* (Ishii et al., 2000) stimulates IP production. MAP kinase activities are elevated through activation of *lpa1* (Erickson et al., 1998), *lpa2* (Bandoh et al., 1999), and *lpa3* (Ishii et al., 2000), although the effects of *lpa1*, *-2*, and *-3* are not identical (Ishii et al., 2000). As LPA and S1P are the natural ligands for LPA receptors and S1P receptors and were tested here in a native preparation, we are not able to pinpoint which receptor subtype(s) are responsible for the observed effects. However, those questions may be addressed

when selective agonists and antagonists become available.

Mobilization of intracellular calcium is a critical cellular response to LPA in many cell types. LPA and S1P, although exhibiting overlapping signaling responses, appear to regulate intracellular calcium signaling in oligodendrocytes differentially. Two types of LPA-induced calcium signal response have been observed in rat mature oligodendrocytes by Fura-2-based single-cell imaging assay (Möller et al., 1999): one with an initial peak and a following decaying plateau (17% out of 71% of responsive cells), another with a persistent plateau (54% out of 71% of responsive cells). As our plate reader-based Fluo-4 assay measured the calcium signals from the total cell population, the kinetics actually reflected the overall response to LPA and, to a certain degree, recapitulated Fura-2-based results. Furthermore, the partial block of LPA effects by PLC inhibitor (U73122) directly demonstrates PLC activation by LPA and supports the notion that LPA-elicited calcium signals in oligodendrocytes are derived from two routes: calcium influx across the plasma membrane and calcium release from internal stores (Möller et al., 1999). These results are also consistent with PLC-dependent LPA-induced calcium response in cell lines stably expressing Edg2 (*lpa1*) and Edg4 (*lpa2*) receptors (An et al., 1998). Similar to pERK activation, LPA-induced $[Ca^{2+}]_i$ increase in oligodendrocytes is not affected by PTX treatment, implying that G-protein subunits other than $G_{i/o}$, and more likely G_q, are involved in LPA-induced calcium signaling. In contrast to two previous studies where S1P was found to increase $[Ca^{2+}]_i$ in rat oligodendrocytes (Hida et al., 1998) and CG4/oligodendrocytes (Fatatis and Miller, 1997), we were unable to demonstrate a measurable $[Ca^{2+}]_i$ increase by S1P with Fluo-4 plate-based assay. The discrepancy could be due to the fact that in the Fura-2-based assay, single cells were used and only 14% (7 out of 50) were responsive to S1P (Hida et al., 1998). Based on the fact the 82% of CG4/oligodendrocytes are responsive to S1P by the same Fura-2-based single-cell imaging assay (Fatatis and Miller, 1997), substantial difference likely exists between native preparation of oligodendrocytes and their CG4 counterparts in terms of S1P response. As our plate reader-based Fluo-4 assay measured the calcium signals from the total cell population, the signals from such a low percentage (if present) might not be detectable.

Oligodendrocytes are susceptible to glutamate-mediated excitatory toxicity in which AMPA receptors play an important role. Our results demonstrated that LPA was unable to prevent AMPA-evoked oligodendrocytes toxicity; therefore, it is unlikely that activation of LPA receptors by their natural ligands will play significant role in protecting AMPA receptor-mediated oligodendrocytes injury.

In conclusion, we demonstrate that LPA and S1P activate the MAPK pathway in oligodendrocytes by coupling to G_q subunits and activation of PLC and PKC pathways. Since cell proliferation and differentiation are the common events downstream of MAPK activation, lpR signaling in health and disease may regulate oligodendrocyte development and differentiation. Therefore, conceptually, lpR ligands have the potential to regulate myelination in vivo and raise the possibility that such ligands may have therapeutic benefit in demyelinating diseases such as MS.

REFERENCES

Allard J, Barron S, Diaz J, Lubetzki C, Zalc B, Schwartz JC, Sokoloff P. 1998. A rat G protein-coupled receptor selectively expressed in myelin-forming cells. Eur J Neurosci 10:1045–1053.

An SZ, Bleu T, Zheng YH, Goetzl EJ. 1998. Recombinant human G protein-coupled lysophosphatidic acid receptors mediate intracellular calcium mobilization. Mol Pharmacol 54:881–888.

An SZ, Zheng YH, Bleu T. 2000. Sphingosine 1-phosphate-induced cell proliferation, survival, and related signaling events mediated by G protein-coupled receptors Edg3 and Edg5. J Biol Chem 275:288–296.

Arimura S, Saito Y, Nakata H, Fukushima K, Nishio E, Watanabe Y. 1998. An EGF receptor-mediated signal attenuates the inhibitory effect of LPA on an adenylate cyclase activity. Life Sci 63:1563–1570.

Bandoh K, Aoki J, Hosono H, Kobayashi S, Kobayashi T, Murakami Murofushi K, Tsujimoto M, Arai H, Inoue K. 1999. Molecular cloning and characterization of a novel human G-protein-coupled receptor, EDG7, for lysophosphatidic acid. J Biol Chem 274:27776–27785.

Bögler O, Wren D, Barnett SC, Land H, Noble M. 1990. Cooperation between two growth factors promotes extended self-renewal and inhibits differentiation of oligodendrocyte-type-2 astrocyte (O-2A) progenitor cells. Proc Natl Acad Sci USA 87:6368–6372.

Buhl AM, Johnson NL, Dhanasekaran N, Johnson GL. 1995. G alpha(12) and G alpha(13) stimulate Rho-dependent stress fiber formation and focal adhesion assembly. J Biol Chem 270:24631–24634.

Canoll PD, Musacchio JM, Hardy R, Reynolds R, Marchionni MA, Salzer JL. 1996. GGF/neuregulin is a neuronal signal that promotes the proliferation and survival and inhibits the differentiation of oligodendrocyte progenitors. Neuron 17:229–243.

Caverzasio J, Palmer G, Suzuki A, Bonjour JP. 2000. Evidence for the involvement of two pathways in activation of extracellular signal-regulated kinase (Erk) and cell proliferation by Gi and Gq protein-coupled receptors in osteoblast-like cells. J Bone Min Res 15:1697–1706.

Cervera P, Tirard M, Barron S, Allard J, Trottier S, Lacombe J, Daumas Duport C, Sokoloff P. 2002. Immunohistological localization of the myelinating cell-specific receptor LP(A1). Glia 38:126–136.

Chun J, Goetzl EJ, Hla T, Igarashi Y, Lynch KR, Moolenaar W, Pyne S, Tigyi G. 2002. International Union of Pharmacology: XXXIV, lysophospholipid receptor nomenclature. Pharmacol Rev 54:265–269.

Contos JJ, Ishii I, Chun J. 2000. Lysophosphatidic acid receptors. Mol Pharmacol 58:1188–1196.

Crespo P, Xu N, Simonds WF, Gutkind JS. 1994. Ras-dependent activation of MAP kinase pathway mediated by G-protein β γ subunits. Nature 369:418–420.

Erickson JP, Wu JJ, Goddard JG, Tigyi G, Kawanishi K, Tomei LD, Kiefer MC. 1998. Edg-2/Vzg-1 couples to the yeast pheromone response pathway selectively in response to lysophosphatidic acid. J Biol Chem 273:1506–1510.

Fatatis A, Miller RJ. 1997. Platelet-derived growth factor (PDGF)-induced Ca^{2+} signaling in the CG4 oligodendroglial cell line and in transformed oligodendrocytes expressing the β-PDGF receptor. J Biol Chem 272:4351–4358.

Fischer DJ, Nusser N, Virag T, Yokoyama K, Wang DA, Baker DL, Bautista D, Parrill AL, Tigyi G. 2001. Short-chain phosphatidates are subtype-selective antagonists of lysophosphatidic acid receptors. Mol Pharmacol 60:776–784.

Gonda K, Okamoto H, Takuwa N, Yatomi Y, Okazaki H, Sakurai T, Kimura S, Sillard R, Harii K, Takuwa Y. 1999. The novel sphingosine 1-phosphate receptor AGR16 is coupled via pertussis toxin-sensitive and -insensitive G-proteins to multiple signalling pathways. Biochem J 337(Pt 1):67–75.

Grey A, Banovic T, Naot D, Hill B, Callon K, Reid I, Cornish J. 2001. Lysophosphatidic acid is an osteoblast mitogen whose proliferative actions involve G(i) proteins and protein kinase C, but not p42/44 mitogen-activated protein kinases. Endocrinology 142:1098–1106.

Handford EJ, Smith D, Hewson L, McAllister G, Beer MS. 2001. Edg2 receptor distribution in adult rat brain. Neuroreport 12:757–760.
Hecht JH, Weiner JA, Post SR, Chun J. 1996. Ventricular zone gene-1 (vzg-1) encodes a lysophosphatidic acid receptor expressed in neurogenic regions of the developing cerebral cortex. J Cell Biol 135: 1071–1083.
Hida H, Takeda M, Soliven B. 1998. Ceramide inhibits inwardly rectifying K^+ currents via a Ras- and Raf-1-dependent pathway in cultured oligodendrocytes. J Neurosci 18:8712–8719.
Hida H, Nagano S, Takeda M, Soliven B. 1999. Regulation of mitogen-activated protein kinases by sphingolipid products in oligodendrocytes. J Neurosci 19:7458–7467.
Hordijk PL, Verlaan I, Vancorven EJ, Moolenaar WH. 1994. protein-tyrosine phosphorylation-induced by lysophosphatidic acid in Rat-1 fibroblasts: evidence that phosphorylation of map kinase is mediated by the Gi-P21ras pathway. J Biol Chem 269:645–651.
Im DS, Fujioka T, Katada T, Kondo Y, Ui M, Okajima F. 1997. Characterization of sphingosine 1-phosphate-induced actions and its signaling pathways in rat hepatocytes. Am J Physiol Gastro Liver Physiol 35:G1091–G1099.
Im DS, Heise CE, Ancellin N, BF OD, Shei GJ, Heavens RP, Rigby MR, Hla T, Mandala S, McAllister G, George SR, Lynch KR. 2000. Characterization of a novel sphingosine 1-phosphate receptor, Edg-8. J Biol Chem 275:14281–14286.
Ishii I, Contos JJA, Fukushima N, Chun J. 2000. Functional comparisons of the lysophosphatidic acid receptors, LP(A1)NVZG-1/EDG-2, LPA2/EDG-4, and LPA3/EDG-7 in neuronal cell lines using a retrovirus expression system. Mol Pharmacol 58:895–902.
Jayadev S, Linardic CM, Hannun YA. 1994. Identification of arachidonic acid as a mediator of sphingomyelin hydrolysis in response to tumor necrosis factor alpha. J Biol Chem 269:5757–5763.
Khorchid A, Larocca JN, Almazan G. 1999. Characterization of the signal transduction pathways mediating noradrenaline-stimulated MAPK activation and c-fos expression in oligodendrocyte progenitors. J Neurosci Res 58:765–778.
Kim MY, Linardic C, Obeid L, Hannun Y. 1991. Identification of sphingomyelin turnover as an effector mechanism for the action of tumor necrosis factor alpha and gamma-interferon: specific role in cell differentiation. J Biol Chem 266:484–489.
Kim JH, Kim JH, Song WK, Kim JH, Chun JS. 2000. Sphingosine 1-phosphate activates Erk-1/-2 by transactivating epidermal growth factor receptor in rat-2 cells. IUBMB Life 50:119–124.
Kim MJ, Lee YS, Han JK. 2000. Modulation of lysophosphatidic acid-induced Cl^- currents by protein kinases A and C in the Xenopus oocyte. Biochem Pharmacol 59:241–247.
Kimura T, Watanabe T, Sato K, Kon J, Tomura H, Tamama K, Kuwabara A, Kanda T, Kobayashi I, Ohta H, Ul M, Okajima F. 2000. Sphingosine 1-phosphate stimulates proliferation and migration of human endothelial cells possibly through the lipid receptors, Edg-1 and Edg-3. Biochem J 348(Pt 1):71–76.
Kon J, Sato K, Watanabe T, Tomura H, Kuwabara A, Kimura T, Tamama K, Ishizuka T, Murata N, Kanda T, Kobayashi I, Ohta H, Ui M, Okajima F. 1999. Comparison of intrinsic activities of the putative sphingosine 1-phosphate receptor subtypes to regulate several signaling pathways in their cDNA-transfected Chinese hamster ovary cells. J Biol Chem 274:23940–23947.
Lee MJ, Van Brocklyn JR, Thangada S, Liu CH, Hand AR, Menzeleev R, Spiegel S, Hla T. 1998. Sphingosine-1-phosphate as a ligand for the G protein-coupled receptor EDG-1. Science 279:1552–1555.
Lee OH, Kim YM, Lee YM, Moon EJ, Lee DJ, Kim JH, Kim KW, Kwon YG. 1999. Sphingosine 1-phosphate induces angiogenesis: its angiogenic action and signaling mechanism in human umbilical vein endothelial cells. Biochem Biophys Res Commun 264:743–750.
Malek RL, Toman RE, Edsall LC, Wong S, Chiu J, Letterle CA, Van Brocklyn JR, Milstien S, Spiegel S, Lee NH. 2001. Nrg-1 belongs to the endothelial differentiation gene family of G protein-coupled sphingosine-1-phosphate receptors. J Biol Chem 276:5692–5699.
Manning TJ, Sontheimer H. 1999. Recording of intracellular Ca^{2+}, Cl^-, pH and membrane potential in cultured astrocytes using a fluorescence plate reader. J Neurosci Meth 91:73–81.
Matute C, SanchezGomez MV, MartinezMillan L, Miledi R. 1997. Glutamate receptor-mediated toxicity in optic nerve oligodendrocytes. Proc Natl Acad Sci USA 94:8830–8835.
McCarthy KD, Vellis JD. 1980. Preparation of separate astroglial and oligodendroglial cultures from rat cerebral tissue. J Cell Biol 85: 890–902.
McDonald JW, Althomsons SP, Hyrc KL, Choi DW, Goldberg MP. 1998. Oligodendrocytes from forebrain are highly vulnerable to AMPA/kainate receptor-mediated excitotoxicity. Nat Med 4:291–297.
Möller T, Musante DB, Ransom BR. 1999. Lysophosphatidic acid-induced calcium signals in cultured rat oligodendrocytes. Neuroreport 10:2929–2932.
Moolenaar WH. 1995. Lysophosphatidic acid signalling. Curr Opin Cell Biol 7:203–210.
Ohata H, Aizawa H, Momose K. 1997. Lysophosphatidic acid sensitizes mechanical stress-induced Ca^{2+} response via activation of phospholipase C and tyrosine kinase in cultured smooth muscle cells. Life Sci 60:1287–1295.
Okamoto H, Takuwa N, Gonda K, Okazaki H, Chang K, Yatomi Y, Shigematsu H, Takuwa Y. 1998. EDG1 is a functional sphingosine-l-phosphate receptor that is linked via a G(i/o) to multiple signaling pathways, including phospholipase C activation, Ca^{2+} mobilization, Ras-mitogen-activated protein kinase activation, and adenylate cyclase inhibition. J Biol Chem 273:27104–27110.
Paolucci L, Sinnett Smith J, Rozengurt E. 2000. Lysophosphatidic acid rapidly induces protein kinase D activation through a pertussis toxin-sensitive pathway. Am J Physiol Cell Physiol 278:C33–C39.
Pébay A, Torrens Y, Toutant M, Cordier J, Glowinski J, Tencé M. 1999. Pleiotropic effects of lysophosphatidic acid on striatal astrocytes. Glia 28:25–33.
Pébay A, Toutant M, Premont J, Calvo CF, Venance L, Cordier J, Glowinski J, Tencé M. 2001. Sphingosine-1-phosphate induces proliferation of astrocytes: regulation by intracellular signalling cascades. Eur J Neurosci 13:2067–2076.
Ramakers GJ, Moolenaar WH. 1998. Regulation of astrocyte morphology by RhoA and lysophosphatidic acid. Exp Cell Res 245:252–262.
Rao TS, Lariosa-Willingham KD, Lin FF, Palfreyman EL, Yu N, Chun J, Webb M. 2003. Pharmacological characterization of lysophospholipid receptor signal transduction pathways in rat cerebrocortical astrocytes. Brain Res (in press).
Rui LY, Archer SF, Argetsinger LS, Carter Su C. 2000. Platelet-derived growth factor and lysophosphatidic acid inhibit growth hormone binding and signaling via a protein kinase C-dependent pathway. J Biol Chem 275:2885–2892.
Sautin YY, Crawford JM, Svetlov SI. 2001. Enhancement of survival by LPA via Erk1/Erk2 and PI 3-kinase/Akt pathways in a murine hepatocyte cell line. Am J Physiol Cell Physiol 281:C2010–C2019.
Seewald S, Schmitz U, Seul C, Ko Y, Sachinidis A, Vetter H. 1999. Lysophosphatidic acid stimulates protein kinase C isoforms α, β, ϵ, and ζ in a pertussis toxin sensitive pathway in vascular smooth muscle cells. Am J Hypertens 12:532–537.
Stankoff B, Barron S, Allard J, Barbin G, Noel F, Aigrot MS, Premont J, Sokoloff P, Zalc B, Lubetzki C. 2002. Oligodendroglial expression of Edg-2 receptor: developmental analysis and pharmacological responses to lysophosphatidic acid. Mol Cell Neurosci 20:415–428.
Stariha RL, Kim SU. 2001. Protein kinase C and mitogen-activated protein kinase signalling in oligodendrocytes. Microsc Res Tech 52:680–688.
Takeda H, Matozaki T, Fujioka Y, Takada T, Noguchi T, Yamao T, Tsuda M, Ochi F, Fukunaga K, Narumiya S, Yamamoto T, Kasuga M. 1998. Lysophosphatidic acid-induced association of SHP-2 with SHPS-1: roles of RHO, FAK, and a SRC family kinase. Oncogene 16:3019–3027.
Takeda H, Matozaki T, Takada T, Noguchi T, Yamao T, Tsuda M, Ochi F, Fukunaga K, Inagaki K, Kasuga M. 1999. PI 3-kinase gamma and protein kinase C-zeta mediate RAS-independent activation of MAP kinase by a G(i) protein-coupled receptor. EMBO J 18:386–395.
Tigyi G, Fischer DJ, Sebok A, Marshall F, Dyer DL, Miledi R. 1996. Lysophosphatidic acid-induced neurite retraction in PC12 cells: neurite-protective effects of cyclic AMP signaling. J Neurochem 66:549–558.
Tokumura A. 1995. A family of phospholipid autacoids: occurrence, metabolism and bioactions. Prog Lipid Res 34:151–184.
van Corven EJ, Hordijk PL, Medema RH, Bos JL, Moolenaar WH. 1993. Pertussis toxin-sensitive activation of p21ras by G protein-coupled receptor agonists in fibroblasts. Proc Natl Acad Sci USA 90:1257–1261.
Weiner JA, Hecht JH, Chun J. 1998. Lysophosphatidic acid receptor gene vzg-1/lp(A1)/edg-2 is expressed by mature oligodendrocytes during myelination in the postnatal murine brain. J Comp Neurol 398:587–598.
Weiner JA, Chun J. 1999. Schwann cell survival mediated by the signaling phospholipid lysophosphatidic acid. Proc Natl Acad Sci USA 96:5233–5238.
Windh RT, Lee MJ, Hla T, An SZ, Barr AJ, Manning DR. 1999. Differential coupling of the sphingosine 1-phosphate receptors Edg-1, Edg-3, and H218/Edg-5 to the G(i), G(q), and G(12) families of heterotrimeric G proteins. J Biol Chem 274:27351–27358.
Zondag GCM, Postma FR, VanEtten I, Verlaan I, Moolenaar WH. 1998. Sphingosine 1-phosphate signalling through the G-protein-coupled receptor Edg-1. Biochem J 330(Pt 2):605–609.